

The Knowable Future: Mapping the Decay of Past–Future Mutual Information Across Forecast Horizons

Peter Maurice Catt

*School of Computing, Electrical and Applied Technology
UNITEC Institute of Technology, Auckland, New Zealand*

Abstract

The ability to assess ex-ante whether a time series is likely to be accurately forecast is important for forecasting practice because it informs the degree of modelling effort warranted. We define forecastability as a property of a time series (given a declared information set), and measure horizon-specific forecastability as the reduction in uncertainty provided by the past, using auto-mutual information (AMI) at lag h . AMI is estimated from training data using a k-nearest-neighbour estimator and evaluated against out-of-sample forecast error (sMAPE) on a filtered, balanced sample of 1,350 M4 series across six sampling frequencies. Seasonal Naïve, ETS, and N-BEATS are used as probes of out-of-sample forecast performance. Training-only AMI provides a frequency-conditional diagnostic for forecast difficulty: for Hourly, Weekly, Quarterly, and Yearly series, AMI exhibits consistently negative rank correlation with sMAPE across probes. Under N-BEATS, the correlation is strongest for Hourly ($\rho = -0.52$) and Weekly ($\rho = -0.51$), with Quarterly ($\rho = -0.42$) and Yearly ($\rho = -0.36$) also substantial. Monthly is probe-dependent (Seasonal Naïve $\rho = -0.12$; ETS $\rho = -0.26$; N-BEATS $\rho = -0.24$). Daily shows notably weaker AMI–sMAPE correlation under this protocol, suggesting limited ability to discriminate between series despite the presence of temporal dependence. The findings support within-frequency triage and effort allocation based on measurable signal content prior to forecasting, rather than between-frequency comparisons of difficulty.

Keywords: Forecastability; predictive information; mutual information; time series; M4 competition; decision analytics; forecast error; forecasting

1. Introduction

Forecasters across domains face collections of time series with varying forecastability. Some series respond well to sophisticated methods. Others show no improvement over simple baselines, regardless of model complexity or computational investment (Makridakis et al., 2018). The practical question is: which series justify sophisticated modelling effort, and which do not?

Current practices rely on trial and error. Practitioners build models, evaluate performance, then refine or abandon approaches based on results. This is operationally inefficient. If a series lacks exploitable structure at relevant horizons, model tuning is unlikely to improve forecasts substantially. Time and resources should be allocated elsewhere or focused on mitigating forecast error impacts rather than reducing errors that cannot be reduced (Kolassa, 2009).

Forecastability assessment should happen before model building begins. The question is whether a series contains predictive information at horizons that matter for decisions. This is a property of the time series itself (given a declared information set), not a property of a particular forecasting model. A series with strong organised patterns is forecastable even if current models perform poorly. Conversely, a series with weak temporal structure is difficult to forecast regardless of method sophistication.

We estimate horizon-specific forecastability and validate it against realised accuracy; we do not claim a universal ‘forecast horizon’ boundary. The goal is operational triage, not theoretical characterisation of forecastability limits.

Classical variability measures like standard deviation or coefficient of variation do not address this. A volatile series with large seasonal swings can be easier to forecast than a smooth series drifting randomly. What matters is not how much a series varies, but how much the past tells us about the

future (Catt, 2009). High variability with strong patterns is forecastable. Low variability with random drift is not.

The challenge is making forecastability operational. We need a measure that can be computed from historical data alone, estimated before forecasting begins, and validated against actual out-of-sample performance. It must handle heterogeneous series lengths and acknowledge that forecastability varies by horizon. A single score ignoring horizon is meaningless (Tiao & Tsay, 1994).

This paper draws on predictive information theory from statistical physics and learning theory (Bialek et al., 2001; Jaynes, 1957). We define forecastability at horizon h as mutual information $I(\text{Past}; \text{Future}_h)$, the reduction in uncertainty about the future obtained by observing the past. High mutual information indicates organised, exploitable structure. Low mutual information indicates weak or unexploitable dependence between past and future observations. We make no assumptions about the underlying data-generating process, which may be latent and time-varying, and instead focus on measurable past–future dependence in the realised data. AMI therefore quantifies an observable consequence of the data-generating mechanism—namely, how much predictive information persists at a given horizon without requiring parametric, structural, or stationarity assumptions about its form.

AMI is interpreted ordinally (rank-based), not metrically; our conclusions depend on whether AMI correctly orders series by forecastability, not on absolute mutual information values or estimator-specific units.

Contributions. This study makes two primary contributions:

1. A pre-modelling triage framework for allocating modelling effort by series and horizon. We provide a practical method for classifying series into action categories (invest in modelling / model cautiously / manage uncertainty) based on ex-ante forecastability assessment. This is the primary contribution for decision support.
2. Empirical validation. We demonstrate that AMI computed from training data correlates with out-of-sample forecast error (sMAPE) in frequency-dependent patterns, validating AMI as a pre-modelling diagnostic. Three probe models (Seasonal Naïve, ETS, N-BEATS) spanning different representational capacities confirm that the relationship holds across model classes, though strength and direction vary.

The methodology is tested on M4 competition series across six frequencies (Makridakis et al., 2020). The goal is not competition performance but decision analytics. The question is not ‘Can we beat benchmark X?’ but ‘Which series justify investment in methods beyond benchmark X?’ This reframes forecasting from a universal accuracy contest to a portfolio optimisation problem. The diagnostic answers not ‘which model is best?’ but ‘is this series worth modelling at all?’

We test AMI as a pre-modelling diagnostic under a fixed-origin, fixed-information protocol; observed associations are empirical and frequency-conditional rather than universal laws of predictability.

The remainder of the paper is organised as follows: Section 2 reviews related work, Section 3 describes the experimental protocol, Section 4 presents the data and models, Section 5 reports the empirical results, Section 6 discusses implications and limitations, and Section 7 concludes.

2. Conceptual Foundations

2.1 The Forecastability Problem

Forecasting competitions from M1 onwards show that simple methods remain competitive on average (Makridakis et al., 1982; Makridakis & Hibon, 2000; Petropoulos et al., 2022). This is sometimes misinterpreted as ‘sophistication doesn’t help’. The correct interpretation is that average forecastability across competition portfolios is moderate. Sophisticated methods excel on high-signal

series but struggle on low-signal series where they overfit noise. Simple methods perform adequately on low-signal series but underperform on high-signal series. The average difference narrows.

This supports rather than contradicts the forecastability thesis. Different series have fundamentally different information content. Method selection should respect this. Applying sophisticated methods to all series wastes resources on those that cannot benefit.

2.2 Existing Approaches and Their Limitations

The forecastability problem has been addressed through statistical, information-theoretic, model-based, and practical approaches, each with distinct strengths and limitations.

Statistical measures. The coefficient of variation ($CV = \sigma/\mu$) is widely used in practice to assess forecast difficulty (Gilliland, 2010), but CV conflates signal and noise. A series with large seasonal swings (high CV) may be easier to forecast than one with small random drift (low CV). Classical measures like autocorrelation functions and spectral decomposition identify structure but do not aggregate information into horizon-specific forecastability scores.

Information-theoretic and spectral approaches. Entropy-based measures quantify regularity and pattern complexity (Pincus 1991). Sample entropy (Richman & Moorman, 2000) measures the likelihood that similar patterns persist, with lower entropy indicating higher predictability. Catt (2014) demonstrated that sample entropy provides useful ex-ante indication of forecast accuracy on M3 data, though subject to limitations with intermittent demand and structural breaks. Goerg (2013) introduced Forecastable component analysis (ForeCA), defining forecastability via spectral entropy, with lower spectral entropy indicating higher forecastability. These measures capture pattern complexity that CV cannot, but they produce single global scores that do not vary by horizon.

Model-based and dynamical systems approaches. In econometrics, predictability is measured through variance decomposition or predictive R^2 (Stock & Watson, 2003). Lyapunov exponents quantify sensitivity to initial conditions in dynamical systems, with positive exponents indicating chaos and limited predictability (Eckmann & Ruelle, 1985). These methods assume deterministic dynamics and require long, high-quality series for reliable estimation.

Practical and empirical approaches. Forecast Value Added (FVA) evaluates forecast performance relative to a simple baseline (Gilliland, 2010). If sophisticated methods cannot beat simple baselines, the series has low forecastability or the methods are poorly specified. FVA has proven valuable in operational contexts for identifying which forecasting activities add value, but it requires actual forecasting attempts and cannot be computed ex-ante from historical data alone.

Limitations of existing approaches. Three practical limitations constrain existing approaches in operational settings. First, horizon-dependence is ignored. Nearly all existing metrics produce single-valued scores (CV , ApEn, SampEn, spectral entropy, Lyapunov exponents). A series highly predictable at 1-step ahead may be unpredictable at 12-steps ahead, or vice versa. The relationship between short-term and long-term forecastability is complex and horizon-specific assessment is essential (Tiao & Tsay, 1994). Second, explicit alignment with forecast horizons is absent. Spectral entropy summarises frequency-domain concentration but does not map directly to h -step-ahead prediction difficulty. Sample entropy provides a global regularity measure but does not specify which horizons benefit from that regularity. Lyapunov exponents indicate long-term predictability horizons in chaotic systems but not specific h -step-ahead difficulty. Third, comprehensive empirical validation is limited. Sample entropy showed promise in initial M3 studies (Catt, 2014) but comprehensive validation across diverse frequencies, horizons, and methods was not performed. Lyapunov exponents require long, well-resolved series to be estimated reliably and tend to perform poorly on the short, sparse series common in business forecasting settings (Wang, Klee, & Roos, 2025). CV continues to be used despite weak theoretical justification and inconsistent empirical support.

Our approach. We address these limitations through horizon-specific auto mutual information (AMI). Spectral entropy measures overall frequency-domain concentration, but AMI at lag τ directly

quantifies dependence between present values and values τ -steps in the past. Unlike entropy or spectral measures, AMI is explicitly indexed to forecast horizon, which is the key object of decision relevance. Sample entropy requires parameter selection, whereas AMI has a well-established non-parametric estimation framework via k-nearest neighbours. ACF captures only linear dependencies, but AMI captures both linear and nonlinear dependencies through its information-theoretic foundation. The key advantage of our framework is explicit lag-horizon mapping: AMI(τ) aligns to τ -step-ahead forecast difficulty. We compute AMI at lags corresponding to each forecast horizon h , making the connection between measurement and prediction operationally transparent. We then validate this framework comprehensively across M4 series, six frequencies, multiple horizons, and three forecasting methods, providing the empirical grounding that previous entropy-based approaches lacked.

2.3 Information-Theoretic Framework

Shannon (1948) defined entropy to quantify uncertainty in random variables:

$$H(X) = -\sum p(x) \log p(x)$$

For time series prediction, the relevant quantity is not marginal entropy $H(\text{Future})$ but conditional entropy $H(\text{Future} | \text{Past})$. The difference is mutual information:

$$I(\text{Past}; \text{Future}) = H(\text{Future}) - H(\text{Future} | \text{Past})$$

This quantity captures the reduction in uncertainty about the future attributable to the past.

For operational implementation, we use auto mutual information (AMI), which quantifies shared information between a time series and its lagged self. At lag τ :

$$\text{AMI}(\tau) = I(X_t; X_{t+\tau}) = H(X_{t+\tau}) - H(X_{t+\tau} | X_t)$$

This is the mutual information between past and future. It measures how much the past tells you about the future. High predictive information means there's signal available to exploit. Entropy and mutual information are not redundant concepts. Two processes can have the same entropy rate but different 'organised structure'. AMI is the information-theoretic generalisation of the autocorrelation function, capturing both linear and nonlinear temporal dependencies (Fraser & Swinney, 1986; Kantz & Schreiber, 2004).

Bialek et al. (2001) formalised this as predictive information. Related constructs in computational mechanics include excess entropy and statistical complexity (Grassberger, 1986; Crutchfield & Feldman, 2003). The framework has deep precedent in physics, neuroscience, and computational theory where prediction and information processing are fundamental concerns (Palmer, 1999).

2.3.1 Forecastability, Exploitability, and Validation

A key distinction must be made between forecastability as dependence and forecastability as exploitability. AMI measures statistical dependence between past and future, a property of the data-generating process that exists independently of any forecasting method. However, whether that dependence translates into reduced forecast error depends on whether the forecasting method can represent and exploit the relevant structure.

AMI is therefore a diagnostic for available dependence, not a guarantee of error reduction under any particular loss function or hypothesis class. We validate AMI against realised sMAPE using Seasonal Naïve, ETS, and N-BEATS as probes of exploitability across different model classes. Where AMI correlates negatively with sMAPE, the dependence is being exploited. Where correlation is weak or absent, the mismatch is itself informative: it may indicate representation limitations (the model cannot capture the dependence structure), nonstationarity (in-sample dependence does not persist out-of-sample), or insufficient sample size (the dependence cannot be reliably estimated or learned).

3. Experimental Protocol

Figure 1 illustrates the single-series forecastability intuition. Panel A shows the train-test split at a single forecast origin. Panel B displays AMI estimated at each lag from training data. Panel C shows sMAPE evaluated post-origin for three probe models. Panel D demonstrates the key relationship: higher AMI corresponds to lower forecast error.

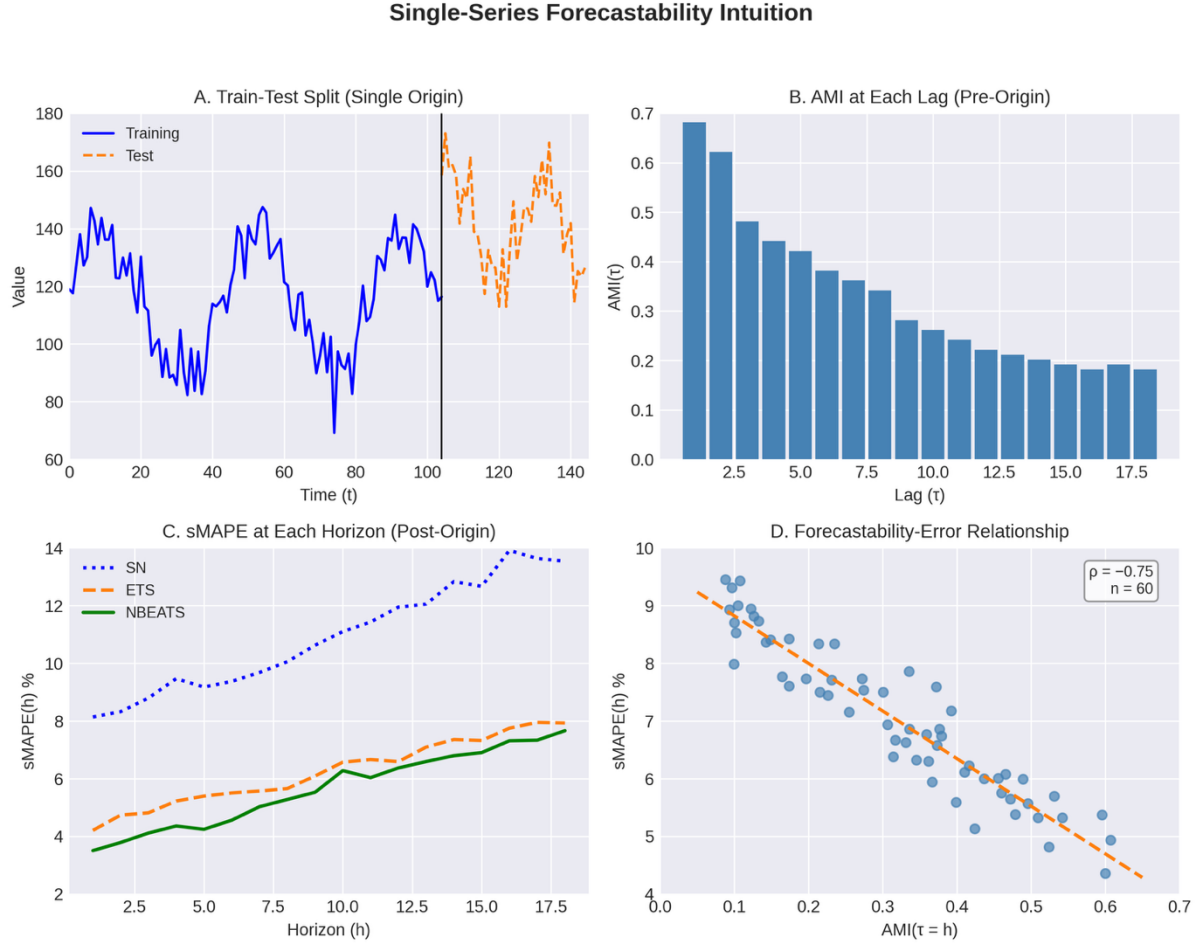


Figure 1. Single-series forecastability intuition. (A) Training and test split at single forecast origin. (B) AMI estimated at each lag from training data. (C) sMAPE evaluated post-origin for three probe models. (D) The key relationship: higher AMI corresponds to lower forecast error.

Figure 2 provides an illustrative view of how horizon-specific auto-mutual information (AMI) behaves under different forms of temporal structure. The examples are included solely to aid interpretation and are not used for model fitting, evaluation, or comparison.

Each row corresponds to a canonical process, with the left panel showing a representative standardised segment of the series for visual context and the right panel showing AMI estimated at increasing horizons using training data only. The processes span deterministic periodic behaviour (sine wave), real seasonal data with noise and trend (AirPassengers), low-dimensional chaotic dynamics (Hénon map), and weakly dependent stochastic behaviour (simulated stock returns).

AMI Illustration Across Canonical Processes

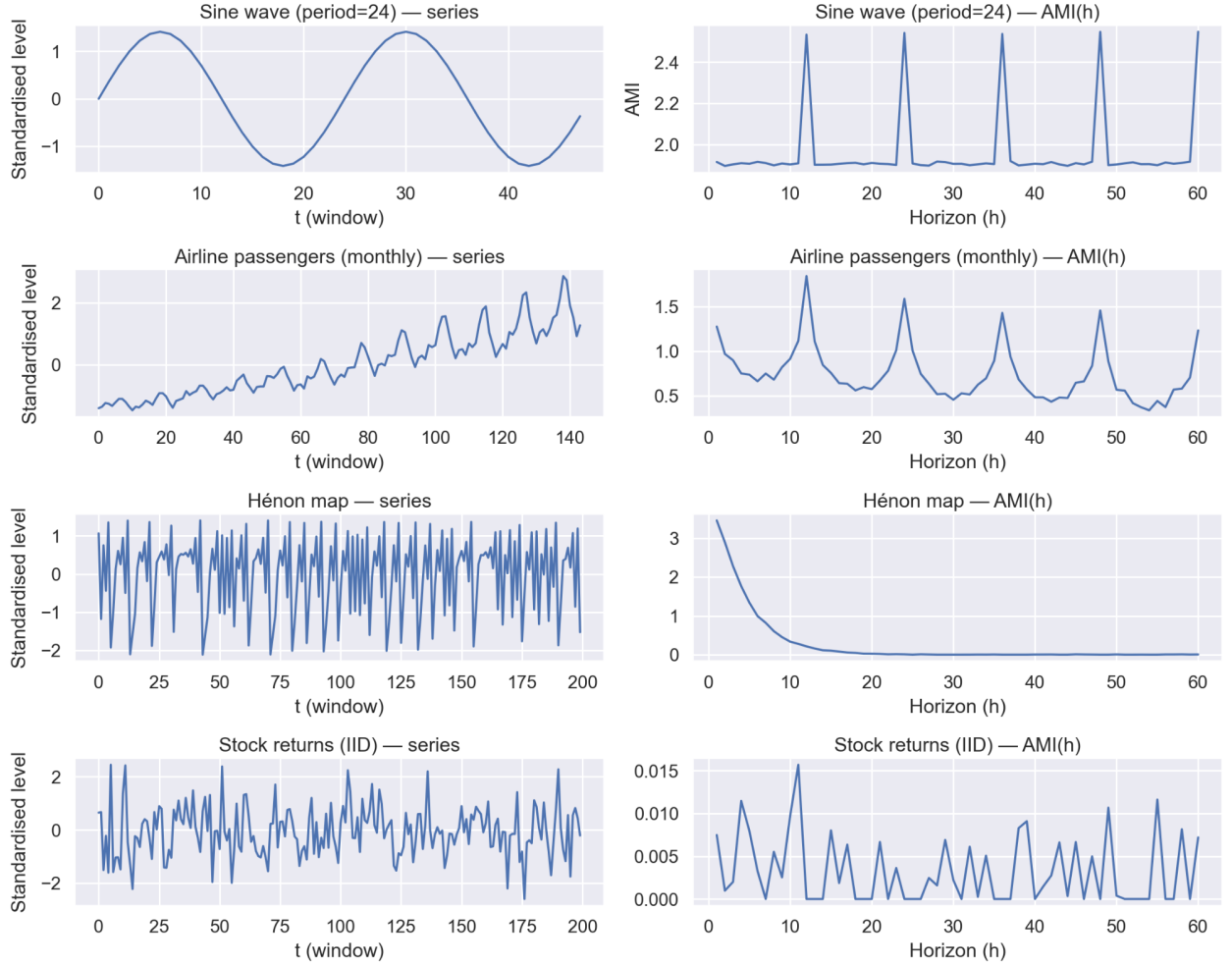


Figure 2. AMI Illustration Across Canonical Processes. Each row shows a representative series segment (left) and horizon-specific AMI profile (right). From top: sine wave (persistent periodic AMI), AirPassengers (seasonal peaks with decay), Hénon map (rapid chaotic decay), simulated stock returns (near-zero AMI). These examples illustrate qualitative AMI behaviour and are not used for model fitting or evaluation.

To make the experimental protocol explicit and to separate pre-modelling diagnostics from post-origin evaluation, we describe the complete forecastability assessment pipeline. Three design choices merit emphasis. First, the protocol iterates over all horizons $h \in H$, computing a separate mutual information estimate at each lag; this traces the decay of past–future dependence as forecast distance increases. Second, AMI estimation uses a k-nearest-neighbour mutual information estimator, which provides consistent estimates for continuous variables without requiring density estimation or binning, a critical advantage over standard Shannon entropy approaches that struggle with real-valued time series. Third, the protocol enforces a single-origin constraint: local models (Seasonal Naïve, ETS) are fitted once per series on Y_{train} , while the global model (N-BEATS) is trained once per frequency on pooled training data; all are then evaluated on Y_{test} without rolling windows or re-fitting, preserving the ex-ante integrity of the AMI diagnostic as a pre-modelling triage tool. The protocol is intentionally asymmetric: diagnostics are computed strictly pre-origin using training data only, and evaluated strictly post-origin against withheld data, preventing any leakage from outcomes into forecastability assessment.

This section describes the complete experimental methodology in sufficient detail for independent replication. All implementations use Python. We define all model specifications, survivorship rules,

evaluation procedures, and forecastability computations. All reported results correspond to run_id = 20260111_174826.

3.1 M4 Dataset Overview

The M4 competition (Makridakis et al., 2020) provides 100,000 time series across six sampling frequencies: Yearly (23,000 series), Quarterly (24,000), Monthly (48,000), Weekly (359), Daily (4,227), and Hourly (414). Series span diverse domains including finance, industry, demographics, and macroeconomics. Each series has a defined training period and a held-out test period whose length varies by frequency: 6 periods for Yearly, 8 for Quarterly, 18 for Monthly, 13 for Weekly, 14 for Daily, and 48 for Hourly.

3.2 Survivor Panel Construction

From the full M4 dataset, we construct survivor panels for each frequency. The target sample sizes are: Hourly (100), Daily (200), Weekly (150), Monthly (300), Quarterly (300), and Yearly (300). These targets balance computational feasibility with statistical power for horizon-specific correlation analysis.

Survivor selection applies two sequential filters.

First, test length feasibility: series must have sufficient observations in the held-out period to evaluate at the worst (maximum) horizon for that frequency. This worst-horizon constraint ensures that all survivors can be evaluated at every required horizon, not just short ones.

Second, AMI feasibility: auto mutual information must be computable at all required lags without numerical failure. Series where kNN estimation fails (typically due to degenerate distributions or insufficient effective sample size) are excluded.

From qualifying series, random stratified sampling by M4 category (Demographic, Finance, Industry, Macro, Micro, Other) is applied where category counts permit. When category counts are insufficient for balanced sampling, available series are included and remaining quota is filled from other categories.

Categories are used for balanced sampling and for checking robustness of the AMI–error relationship across semantic domains; the study is not designed to estimate causal or structural category effects, and we do not claim that categories drive forecastability.

Selection bias acknowledgement. Survivor panels represent the subset of series where AMI and sMAPE are numerically meaningful; results should not be interpreted as population averages over all M4 series. The feasibility filters necessarily exclude degenerate, extremely short, or numerically unstable series. This is appropriate for a diagnostic tool, since forecastability assessment is only meaningful where both the diagnostic and the forecast error metric can be reliably computed. Readers should note that the most problematic series (intermittent demand, near-constant, extremely short) are excluded by design. This is intentional: a diagnostic that cannot be computed reliably on a series cannot support pre-modelling decisions for that series; feasibility is part of operational applicability, not a limitation.

3.3 Forecast Origin and Horizon Structure

Forecasts are generated using a single fixed origin: the last observation of the official M4 training period. No rolling origins or expanding windows are used. This design choice reflects operational forecasting practice where a single forecast must be issued, and avoids the computational complexity of origin-averaging. The trade-off is that single-origin evaluation has higher variance than rolling-origin averages; however, rolling origins would change the decision framing (from “one-shot triage” to “average behaviour over time”) and risk information leakage if not carefully implemented. Rolling-origin robustness is left for future work and is not required for diagnostic validity at the portfolio level, where individual-series variance averages out. This design is conservative for detecting

correlation because single-origin adds noise to the error signal; any relationship that survives is therefore not an artefact of origin averaging.

For each series, forecasts are generated at all horizons from $h = 1$ to $h = H$, where H is the M4-specified test length for that frequency. Performance is evaluated separately at each horizon to enable horizon-specific analysis of forecastability relationships.

3.4 Seasonal Naïve Baseline

Seasonal Naïve (SN) repeats the observation from the same seasonal position one cycle earlier. Formally:

$$\hat{y}_{t+h|t} = y_{t+h-km} \quad \text{where } k = \lceil h/m \rceil$$

This repeats the corresponding seasonal value from the most recent complete cycle, where m is the seasonal period (12 for Monthly, 4 for Quarterly, 52 for Weekly, 7 for Daily, 24 for Hourly). For Yearly data where no seasonal cycle exists, the last observed value is repeated (equivalent to Naïve).

Seasonal Naïve serves as a benchmark representing minimal modelling effort.

3.5 ETS Specification

ETS forecasts are generated using the exponential smoothing state space framework, with automatic selection over additive and damped trend components and additive or multiplicative seasonality where admissible, using information criteria for model choice. The implementation uses `statsmodels.tsa.holtwinters.ExponentialSmoothing` (Seabold & Perktold, 2010).

Multiplicative seasonality is permitted only when all observations are strictly positive. Box-Cox transformation is disabled to maintain interpretability and avoid numerical instability on diverse series.

The seasonal period is set to the M4-specified value for each frequency (12 for Monthly, 4 for Quarterly, 52 for Weekly, 7 for Daily, 24 for Hourly). For Yearly data where no seasonal cycle exists, the model reduces to non-seasonal exponential smoothing with trend selection. We use fixed seasonal periods for comparability across series; unlike M4's Naïve 2 benchmark, we do not conditionally test for seasonality.

Point forecasts are generated for all horizons $h = 1, \dots, H$ from the selected model.

3.6 N-BEATS Specification

N-BEATS (Neural Basis Expansion Analysis for Time Series; Oreshkin et al., 2020) is implemented using the `neuralforecast` library (Olivares et al., 2022). A single global model is trained per frequency on a pooled panel of series and then applied to generate forecasts for all survivor series in that frequency. The trained global model is applied using fixed-origin evaluation (no test-period updating).

Training uses MAE loss with generic stacks; early stopping is disabled to ensure full convergence. A synthetic daily timeline is used for all frequencies to prevent datetime overflow with high-frequency data. Monthly N-BEATS `input_size` was constrained to exceed the seasonal period (12) in all runs, so the Monthly pattern is not attributable to inadequate seasonal context. The key property for our purposes is that N-BEATS represents a fundamentally different model class from ETS (global, nonlinear, and neural), enabling tests of whether AMI-sMAPE relationships are robust across architectures.

3.7 Forecast Error Metric: sMAPE

Symmetric Mean Absolute Percentage Error (sMAPE) is used throughout. For a single series at horizon h :

$$\text{sMAPE}(h) = \frac{2|y_{t+h} - \hat{y}_{t+h|t}|}{|y_{t+h}| + |\hat{y}_{t+h|t}|}$$

sMAPE is bounded between 0 and 2 (or 0% to 200%), scale-independent, and symmetric in over- and under-prediction. It avoids the infinite values that can occur with standard MAPE when actuals approach zero and the scaling issues that arise with MASE on very short series (Hyndman & Koehler, 2006). We report sMAPE as a percentage (i.e., $\text{sMAPE} \times 100$) in all tables and figures.

3.8 AMI Computation

Auto mutual information is computed using a k-nearest-neighbour mutual information estimator implemented via `mutual_info_regression` (scikit-learn), which belongs to the Kraskov-style family of kNN MI estimators (Kraskov et al., 2004). The estimator provides consistent estimates without requiring explicit density estimation or binning, though it exhibits finite-sample bias that increases with dimensionality and decreases with sample size. Our inference relies on rank association (Spearman ρ), reducing sensitivity to monotone estimator bias; conclusions depend on AMI correctly ranking series by forecastability, not on absolute MI values.

AMI is computed on the standardised training history (level series, z-scored). For each series and each horizon h from 1 to H , we compute $\text{AMI}(h)$ as the mutual information between y_{t+h} and $y_{t+h|t}$ using all available training-window pairs. This produces a vector of forecastability values aligned to the horizons at which forecasts are evaluated.

The kNN parameter is set to $k = 8$, fixed globally across all frequencies and horizons for reproducibility. Series where AMI estimation fails at any required lag (typically due to degenerate distributions or insufficient effective sample size) are excluded during survivor selection.

Interpretation note. These are relative AMI estimates used for ranking and triage, not absolute information values in nats or bits. Short-series bias is mitigated by the minimum effective sample size requirement in survivor filtering; remaining bias is addressed by relying on Spearman correlations (robust to monotonic distortions) and stratified analyses rather than absolute AMI magnitudes.

Reproducibility. All reported results correspond to a single deterministic run (`run_id: 20260111_174826`). The code archive includes survivor selection scripts with explicit random seeds, AMI computation routines, forecast generation code for all three probe models, and evaluation scripts. Survivor panel construction is fully reproducible given the M4 dataset and the documented selection rules. No hyperparameter search or model selection was performed post-hoc; all specifications were fixed before evaluation.

4. Data Description

4.1 M4 Dataset Structure and Survivor Selection

The M4 competition dataset contains 100,000 time series across six frequencies. Table 1 summarises the dataset structure and survivor selection outcomes.

Table 1: Dataset Composition and Survivor Selection

Frequency	Total M4	Eligible (approx.)	Target	Selected
Hourly	414	~380	100	100
Daily	4,227	~3,950	200	200
Weekly	359	~340	150	150
Monthly	48,000	~42,000	300	300
Quarterly	24,000	~21,000	300	300
Yearly	23,000	~18,000	300	300

Notes: Eligible counts are approximate, computed after length filters.

The binding constraint varies by frequency. For Weekly, the small M4 pool (359 series) limits available survivors. For Monthly and Quarterly, AMI feasibility is the primary filter. Yearly requires evaluation of approximately 1,010 series to obtain 300 survivors, with AMI infeasibility as the main exclusion mechanism.

5. Results

This section reports empirical findings from the experimental protocol described in Section 3. We present sample coverage, the relationship between forecastability measures (AMI) and realised forecast error (sMAPE), robustness analysis by training length, and decision utility of AMI-based triage.

5.1 Sample Coverage

The survivor panels achieved their targets: Hourly ($n = 100$), Daily ($n = 200$), Weekly ($n = 150$), Monthly ($n = 300$), Quarterly ($n = 300$), and Yearly ($n = 300$). Total survivors across frequencies is 1,350 series. All three models (Seasonal Naïve, ETS, and N-BEATS) produced forecasts at all horizons for the survivor series included in the reported analyses.

5.2 Probe Model Context

Before examining the core AMI-sMAPE relationship, we briefly characterise the probe models to establish that they span different representational capacities and that subsequent results are not artefacts of a particular forecasting architecture. Probe models are used to test whether forecastability rankings persist across model capacity, not to compete for best accuracy; relative probe performance is incidental to the diagnostic question.

Probe models differ in absolute accuracy by frequency: N-BEATS achieves lowest median sMAPE at high frequencies (Hourly, Daily, Weekly), while ETS is competitive at lower frequencies (Quarterly, Yearly). Seasonal Naïve serves as a minimal-complexity baseline throughout. Daily can still have low median error while exhibiting weak cross-series discrimination by AMI.

Across all frequencies, forecast error increases monotonically with horizon (Figure 3), confirming that horizon itself drives forecast difficulty.

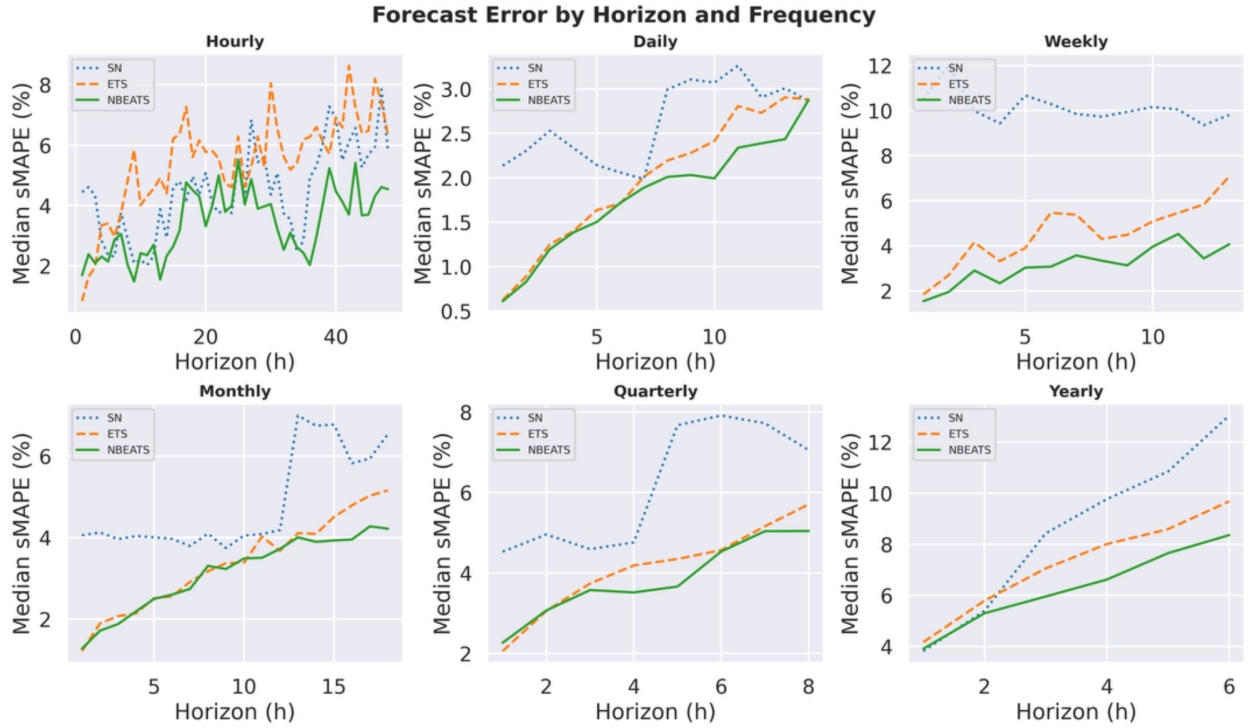


Figure 3. Realised forecast difficulty by horizon and frequency. Each panel shows median sMAPE as a function of forecast horizon h . Error increases monotonically with horizon across all frequencies, with the rate of degradation varying by temporal resolution. Horizon axes reflect frequency-specific test periods (Hourly 1–48, Daily 1–14, Weekly 1–13, Monthly 1–18, Quarterly 1–8, Yearly 1–6).

5.3 Forecastability Measures and Realised Error

A clarification is essential before presenting results. We do not estimate which frequency is harder overall (absolute difficulty); we estimate whether AMI ranks series within a frequency by forecast difficulty at that frequency's horizons (cross-series discrimination). The contribution is within-frequency triage, not between-frequency difficulty rankings.

Figure 4 illustrates the decay of forecastability (AMI) with horizon. Auto-mutual information profiles computed on training data exhibit systematic decay with lag across all frequencies, consistent with diminishing past–future dependence as forecast distance increases. Lag axes reflect frequency-specific horizon ranges. This decay confirms that forecastability is inherently horizon-specific, reinforcing the need for horizon-aligned diagnostics.

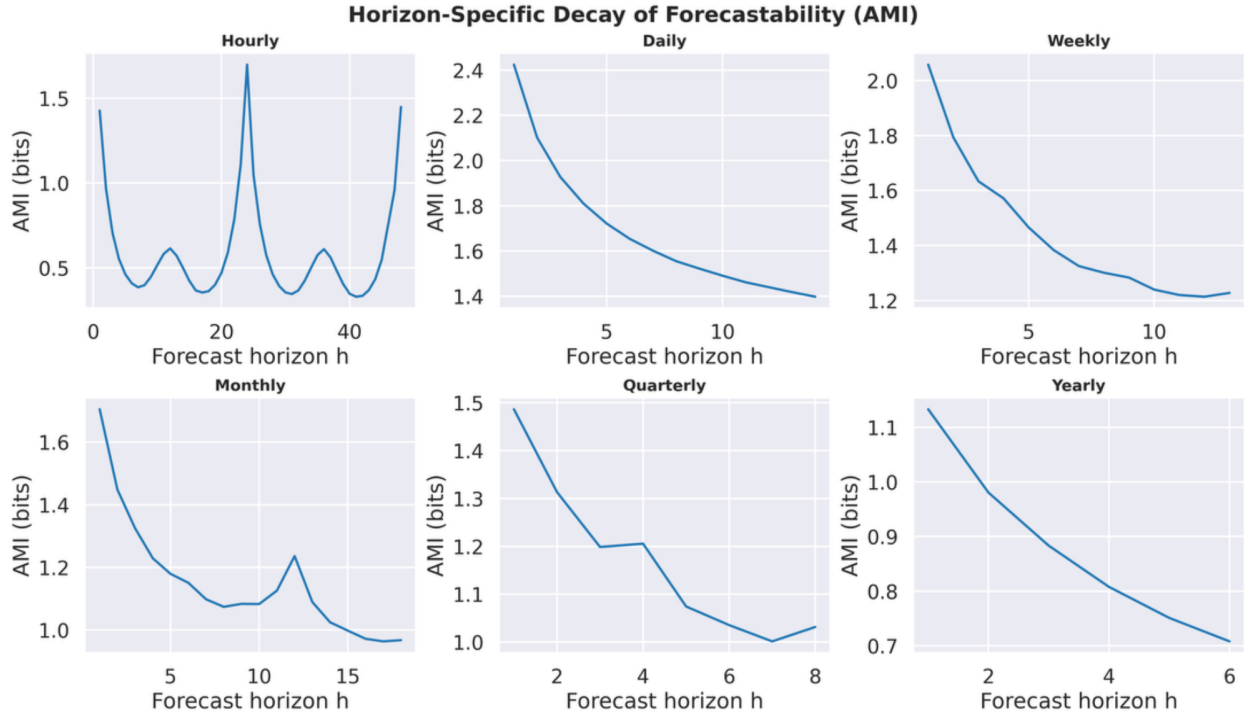


Figure 4. *AMI decay with horizon.* Auto-mutual information profiles computed on training data exhibit systematic decay with lag across all frequencies, consistent with diminishing past–future dependence as forecast distance increases. Lag axes reflect frequency-specific horizon ranges.

The AMI–sMAPE relationship varies systematically by frequency, with strong negative associations at some frequencies and near-zero associations at others. We assess whether AMI behaves as an operational measure of forecastability by examining Spearman rank correlations between AMI and sMAPE. The objective is not strong linear association but stable ordinal separation sufficient for triage decisions.

Table 2: Forecastability–Accuracy Relationship (AMI Validation)

Frequency	Seasonal Naïve	ETS	N-BEATS
Hourly	-0.31	-0.29	-0.52
Daily	0.01	-0.05	-0.07
Weekly	-0.24	-0.57	-0.51
Monthly	-0.12	-0.26	-0.24
Quarterly	-0.27	-0.40	-0.42
Yearly	-0.20	-0.31	-0.36

Notes: Spearman rank correlation computed per horizon across survivor series, then averaged across horizons within each (frequency, model).

Robustness check: conclusions are unchanged when (i) pooling all horizons per frequency and computing a single ρ (pooled Weekly N-BEATS $\rho = -0.47$, pooled Hourly N-BEATS $\rho = -0.55$, confirming the horizon-averaged values), or (ii) reporting median ρ across horizons rather than the mean. The horizon-averaging approach in Table 2 does not mask systematic reversals at specific horizons.

For Hourly, Weekly, Quarterly, and Yearly series, horizon-specific AMI exhibits consistently negative rank association with out-of-sample sMAPE across all probe models. With N-BEATS (highest-capacity probe), the relationship is strongest for Hourly ($\rho = -0.52$) and Weekly ($\rho = -0.51$), with Quarterly ($\rho = -0.42$) and Yearly ($\rho = -0.36$) also substantial. Monthly exhibits a model-dependent pattern: low association with Seasonal Naïve ($\rho = -0.12$) but moderate association with ETS ($\rho = -0.26$) and N-BEATS ($\rho = -0.24$), suggesting dependence that simple methods fail to exploit. Daily frequency constitutes a boundary condition with near-zero correlations across all probes and non-monotone tercile ordering. Note that these results concern cross-series discrimination (AMI ranking series within frequency), not absolute difficulty (median error by frequency). The frequency-level patterns are consistent with M4 competition observations that model performance varies systematically by frequency, but our contribution is the within-frequency ranking, not replication of between-frequency difficulty rankings.

Daily frequency behaves as an empirical boundary condition: although within-series temporal dependence exists, it does not translate into reliable cross-series discrimination of forecast error under the present protocol. We return to this finding in Discussion.

Figure 5 presents a heatmap showing the Spearman correlation between AMI and sMAPE by frequency and horizon. Blue cells indicate negative correlation (higher AMI associated with lower error), confirming that AMI serves as a consistent forecastability indicator for most frequencies, with Daily exhibiting weak and non-monotone association. The contribution lies in ordinal separation for triage, not linear predictability.

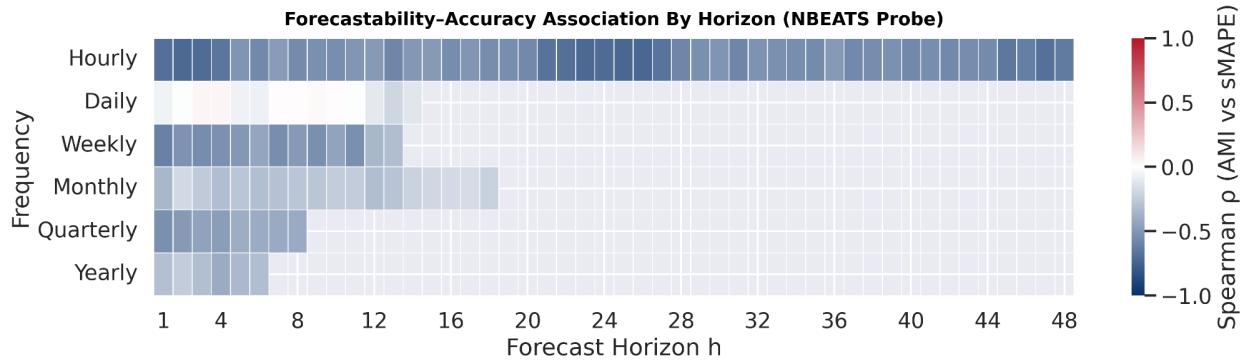


Figure 5. Forecastability-Accuracy Association by Frequency and Horizon (N-BEATS). Spearman correlation (ρ) between AMI and sMAPE by frequency and horizon (N-BEATS probe). Each cell shows series-level Spearman ρ computed across all survivor series within each (frequency, horizon) combination; blue indicates negative correlation (higher AMI associated with lower error). Cells are shown only for horizons defined for each frequency (Hourly 1–48, Daily 1–14, Weekly 1–13, Monthly 1–18, Quarterly 1–8, Yearly 1–6); blank regions are not missing data.

Role of categories relative to frequency. Series categories are incorporated primarily to ensure balanced sampling and to check robustness against dominance by any single domain. To assess whether semantic domain materially alters the relationship between dependence and forecast difficulty, we examined the direction of the AMI–sMAPE association within categories for each frequency. Across frequencies, we do not observe systematic category-level sign reversals relative to the corresponding frequency-level pattern. While association strength varies across categories and statistical power is limited in some cells (notably for Weekly series), the direction of association is broadly consistent. Accordingly, category is treated as a secondary conditioning dimension: forecastability is shaped primarily by temporal resolution and forecast horizon, with semantic domain playing a supporting rather than dominant role.

5.4 Robustness: Training Length Effects

A natural concern is whether AMI-sMAPE correlations are confounded by series length. Stratified analysis within each frequency shows that negative correlations persist across all length terciles (Table 3), indicating that the forecastability signal is not merely a proxy for series length. We report tercile stratification for the global probe (N-BEATS) as an illustrative check; results are qualitatively similar for ETS.

Table 3: AMI-sMAPE Correlations by Training Length Tercile (N-BEATS)

Frequency	Short	Medium	Long
Weekly	-0.52	-0.55	-0.54
Monthly	-0.23	-0.20	-0.19
Yearly	-0.31	-0.28	-0.27

Notes: Series are stratified into terciles by training length within each frequency. Values are Spearman ρ between AMI and sMAPE within each tercile. N-BEATS reported as an illustrative global probe; ETS shows qualitatively similar patterns.

5.5 Decision Utility of Forecastability Assessment

The practical value of forecastability assessment lies in its ability to inform resource allocation decisions before forecasting begins. Table 4 demonstrates this by showing median sMAPE conditional on AMI terciles.

Table 4: Decision Utility — Median sMAPE by AMI Tercile

Frequency	SN Low	SN Mid	SN High	ETS Low	ETS Mid	ETS High	NB Low	NB Mid	NB High
Hourly	7.98	5.07	1.16	9.85	7.59	0.55	6.84	3.67	0.63
Daily	2.93	2.31	2.68	2.41	1.64	1.55	2.29	1.40	1.44
Weekly	11.60	9.91	7.42	11.33	4.27	1.78	6.99	3.25	1.26
Monthly	5.08	4.30	3.15	4.17	3.11	1.66	5.21	4.37	3.41
Quarterly	8.40	6.19	4.41	7.16	4.46	2.03	6.82	4.18	1.77
Yearly	10.61	9.41	6.03	10.59	7.82	4.49	10.72	6.94	3.83

Notes: AMI terciles computed within each frequency across all valid (series, horizon) pairs. Values are median sMAPE (%).

For five of six frequencies, median sMAPE decreases monotonically from Low to High AMI terciles. The gradient is steepest for Hourly (94.4%) and Weekly (84.3%), indicating that AMI-based triage delivers substantial discrimination, functioning as a decision-relevant frontier rather than a predictive model diagnostic. For the remaining frequencies, the tercile ordering (Low \geq Medium \geq High) confirms that weak rank correlations do not invalidate AMI as a screening mechanism, as decision usefulness depends on ordinal separation rather than pointwise accuracy. This demonstrates operational value across most frequencies, with strength varying by data characteristics.

In operational terms, Low-AMI series warrant baseline forecasting with emphasis on consequence mitigation rather than accuracy improvement; High-AMI series justify investment in model development, tuning, and monitoring; Medium-AMI series require cautious modelling with capped expectations and robust fallback procedures.

6. Discussion

6.1 The AMI–Error Relationship is Frequency-Conditional

The dominant finding of this study is that the AMI–sMAPE relationship is strongly frequency-conditional. At Hourly, Weekly, Quarterly, and Yearly frequencies, AMI computed from training data provides a valid diagnostic signal for out-of-sample forecast difficulty across all probe models. Monthly frequency exhibits an intermediate pattern where signal emerges only with sophisticated methods. For Daily series, AMI indicates non-trivial past–future dependence, but its rank association with realised sMAPE is materially weaker than for other frequencies under the present protocol, implying reduced discriminative power for within-frequency triage.

This finding establishes an operational constraint for AMI-based triage: the diagnostic should be validated within each application context rather than assumed universal. These observed associations are empirical and protocol-specific rather than universal laws of predictability.

6.2 Daily frequency: dependence present, weaker discriminative power

Daily series show substantial past–future dependence (AMI) in absolute terms, yet forecast error is low in absolute terms across the probe models. Consistent with this compression of error, the AMI–sMAPE association is weaker for Daily than for most other frequencies: variation in AMI provides limited discrimination among already accurate series, even though dependence itself is clearly present. This should be read as a frequency-conditional limitation on the triage value of AMI for Daily under the present fixed-origin evaluation protocol, not as evidence that temporal dependence is absent.

6.3 Forecastability versus Exploitability

A conceptual distinction is necessary. *Forecastability* as we define it, namely AMI between past and future, is a property of the series itself, independent of any forecasting model. It measures statistical dependence in the data-generating process. *Exploitability* is the degree to which a particular model class can convert that dependence into accurate forecasts.

AMI measures total dependence; the fraction that translates to error reduction depends on the model’s hypothesis class. At Weekly frequency, all probes are negative, with ETS strongest ($\rho = -0.57$), followed by N-BEATS ($\rho = -0.51$), and Seasonal Naïve weaker ($\rho = -0.24$).

This pattern, where different probe models exhibit varying correlation strengths against the same underlying dependence, confirms that exploitability is model-dependent while forecastability is not.

6.4 Moderating Factors

Beyond frequency and horizon, several factors moderate the forecastability-accuracy relationship. Series length affects both AMI estimation variance and the training signal available to statistical and neural models; shorter series yield noisier diagnostics and less reliable forecasts regardless of method. Seasonal strength matters because stable, repeating patterns benefit structured models like ETS and even Seasonal Naïve, whereas weak or evolving seasonality favours more flexible approaches. Variance structure and scale effects may also influence the AMI-sMAPE relationship, though this study did not directly test these dimensions.

Structural breaks and regime instability present a more fundamental challenge, as they can sever the link between in-sample dependence and out-of-sample difficulty. Since we treat the data-generating process as latent and measure only its observable consequence (past-future dependence in the realised training segment), forecastability diagnostics are inherently conditional on the assumption that the future segment is governed by a similar process. When regimes shift, historical dependence patterns may not persist. Finally, cross-series heterogeneity affects global models: pooled learning benefits

portfolios with shared structure but offers diminishing returns when series are fundamentally dissimilar.

This study explicitly tested frequency, horizon, and series length effects. Seasonal strength, variance structure, and regime stability remain avenues for future investigation.

6.5 Implications for Multivariate Forecasting

Although the empirical analysis focuses on univariate series, the findings carry direct implications for multivariate forecasting contexts. The use of global models introduces a form of implicit multivariate learning by exploiting shared structure across a large panel of series, without requiring explicit specification of cross-series dependencies. Our results suggest that forecastability is primarily governed by temporal resolution and effective information content within individual series, which implies that univariate forecastability is a necessary, though not sufficient, condition for value creation in multivariate models.

This leads to a practical gating rule: multivariate enrichment should be attempted only when univariate forecastability is low but plausible external drivers exist at the decision horizon. If univariate AMI is already high, covariates are unlikely to add value because the target series already contains sufficient predictive structure. Conversely, if univariate AMI is low and no leading indicators exist, covariates will not rescue an inherently unforecastable target. A related consideration is measurement cadence: low-frequency series are unlikely to benefit from covariates unless those covariates are measured at higher cadence and genuinely lead the target. Annual series paired with annual covariates simply compound information scarcity.

6.6 Implications for Decision Workflows

These findings support a concrete pre-modelling diagnostic workflow. Before committing forecasting resources, practitioners should first identify the temporal resolution and decision-relevant horizon, since frequency determines baseline expectations for forecastability. The AMI-sMAPE relationship is strongest for Weekly and remains substantial for Hourly and Quarterly. Next, AMI should be computed at relevant lags, noting training series length as a moderating factor.

Based on frequency, AMI level, and series characteristics, each series can then be assigned to an appropriate modelling regime. Series with high AMI at Weekly or Hourly frequency warrant investment in more sophisticated models such as ETS or global neural architectures, where the strong negative AMI-sMAPE correlations (Table 2) indicate meaningful accuracy gains over simple baselines. Series in the middle AMI tercile, or at Monthly and Quarterly frequencies, merit standard models with managed horizon expectations; ensemble or robustified approaches may be appropriate. Series with low AMI or unstable AMI estimation are better served by simple baselines. For these series, resources should shift from forecast refinement toward consequence mitigation: safety stock sizing, scenario planning, cadence adjustment, or decision architectures that are robust to forecast error.

This workflow operationalises the core finding: forecastability assessment should precede model selection, and the appropriate action depends on both frequency and measured dependence strength.

6.7 Limitations and Future Research

Several limitations warrant acknowledgement. Survivorship filtering was necessary to compute AMI reliably, which means that forecastability assessment is only meaningful where it is definable. The method is best framed as a ‘feasible where definable’ triage tool rather than a universal measure applicable to all series.

Validation used three specific forecasting methods on M4 data. While the conceptual framework is general, empirical relationships are context-dependent, and domain-specific validation remains essential before operational deployment. This study also focuses exclusively on point forecast

accuracy measured via sMAPE; probabilistic forecasting, density forecast evaluation, and decision-theoretic loss functions may exhibit different relationships with AMI.

Finally, horizon-specific forecastability is conditioned on the realised DGP segment observed in the training window. If the underlying data-generating process changes between estimation and forecast periods, in-sample dependence will not predict out-of-sample difficulty.

7. Conclusions and Recommendations

This study developed and validated an information-theoretic framework for assessing time series forecastability. The central finding is that AMI provides a pre-modelling diagnostic whose strength is frequency and probe-conditional. For Hourly, Weekly, Quarterly, and Yearly series, horizon-specific AMI exhibits consistently negative rank association with out-of-sample sMAPE across all probe models. Monthly exhibits a probe-dependent pattern: the AMI–sMAPE association is weak under Seasonal Naïve but stronger under ETS and N-BEATS, indicating that dependence detected in training data may not translate into accuracy improvements for simpler seasonal baselines. Daily shows materially weaker AMI–sMAPE association than most other frequencies under the present fixed-origin protocol, implying reduced discriminative power for within-frequency triage despite the presence of temporal dependence.

The AMI–sMAPE relationship is frequency-conditional, which carries an operational implication: AMI-based triage should be validated within each application context rather than assumed universal. A conceptual distinction between forecastability and exploitability is useful for interpretation. AMI measures horizon-specific past–future dependence in the realised series, while exploitability, the extent to which this dependence can be converted into low forecast error, depends on the forecasting method class and evaluation protocol. Consistent with this distinction, association magnitudes vary across probes, with ETS and N-BEATS generally exhibiting stronger rank associations than Seasonal Naïve.

For practitioners, these findings suggest a clear sequence: stratify by frequency first; compute AMI as a screening signal to rank series by expected difficulty within a frequency; prioritise sophisticated modelling where AMI indicates stronger dependence and where the chosen method class is able to exploit that dependence; and recognise cases where diagnostics provide limited discrimination, shifting effort from marginal model refinement toward decision robustification when signal is weak.

For researchers, several avenues merit investigation: identifying the conditions under which Daily series yield weak AMI–error discrimination under fixed-origin protocols; extending validation to probabilistic forecasting and decision-theoretic loss functions; exploring multivariate extensions in which univariate forecastability gates covariate inclusion; and quantifying the roles of series length, scale, and sampling design across additional datasets.

The central contribution of this study is not a new forecasting algorithm but a diagnostic layer that can precede model selection. Forecastability assessment addresses a practitioner-critical question: not “which model is best?”, but “is this series worth modelling at all?”. Horizon-specific diagnostics provide a low-cost screening layer that helps allocate forecasting effort before modelling begins.

References

Bialek, W., Nemenman, I., & Tishby, N. (2001). Predictability, complexity, and learning. *Neural Computation*, 13(11), 2409–2463.

Catt, P. M. (2009). Forecastability: Insights from physics, graphical decomposition, and information theory. *Foresight: The International Journal of Applied Forecasting*, 13, 24–33.

Catt, P. M. (2014). Entropy as an a priori indicator of forecastability [Working paper]. ResearchGate.

Cover, T. M., & Thomas, J. A. (2006). *Elements of information theory* (2nd ed.). Wiley.

Crutchfield, J. P., & Feldman, D. P. (2003). Regularities unseen, randomness observed: Levels of entropy convergence. *Chaos*, 13(1), 25–54.

Delgado-Bonal, A., & Marshak, A. (2019). Approximate entropy and sample entropy: A comprehensive tutorial. *Entropy*, 21(6), 541.

Eckmann, J.-P., & Ruelle, D. (1985). Ergodic theory of chaos and strange attractors. *Reviews of Modern Physics*, 57(3), 617–656.

Fraser, A. M., & Swinney, H. L. (1986). Independent coordinates for strange attractors from mutual information. *Physical Review A*, 33(2), 1134–1140.

Gilliland, M. (2010). *The business forecasting deal*. Wiley.

Goerg, G. M. (2013). Forecastable component analysis. In *Proceedings of the 30th International Conference on Machine Learning* (pp. 64–72). PMLR.

Grassberger, P. (1986). Toward a quantitative theory of self-generated complexity. *International Journal of Theoretical Physics*, 25(9), 907–938.

Hyndman, R. J., & Koehler, A. B. (2006). Another look at measures of forecast accuracy. *International Journal of Forecasting*, 22(4), 679–688.

Jaynes, E. T. (1957). Information theory and statistical mechanics. *Physical Review*, 106(4), 620–630.

Kantz, H., & Schreiber, T. (2004). *Nonlinear time series analysis* (2nd ed.). Cambridge University Press.

Kolassa, S. (2009). Can we obtain valid benchmarks from published surveys of forecast accuracy? *Foresight: The International Journal of Applied Forecasting*, 14, 6–12.

Kraskov, A., Stögbauer, H., & Grassberger, P. (2004). Estimating mutual information. *Physical Review E*, 69(6), 066138.

Makridakis, S., & Hibon, M. (2000). The M3-competition: Results, conclusions and implications. *International Journal of Forecasting*, 16(4), 451–476.

Makridakis, S., Andersen, A., Carbone, R., Fildes, R., Hibon, M., Lewandowski, R., Newton, J., Parzen, E., & Winkler, R. (1982). The accuracy of extrapolation (time series) methods: Results of a forecasting competition. *Journal of Forecasting*, 1(2), 111–153.

Makridakis, S., Spiliotis, E., & Assimakopoulos, V. (2018). The M4 competition: Results, findings, conclusion and way forward. *International Journal of Forecasting*, 34(4), 802–808.

Makridakis, S., Spiliotis, E., & Assimakopoulos, V. (2020). The M4 competition: 100,000 time series and 61 forecasting methods. *International Journal of Forecasting*, 36(1), 54–74.

Olivares, K. G., Challu, C., Marcjasz, G., Weron, R., & Dubrawski, A. (2022). NeuralForecast: User-friendly state-of-the-art neural forecasting models. In *Proceedings of the 21st Python in Science Conference* (pp. 1–9). <https://github.com/Nixtla/neuralforecast>.

Oreshkin, B. N., Carpow, D., Chapados, N., & Bengio, Y. (2020). N-BEATS: Neural basis expansion analysis for interpretable time series forecasting. In *International Conference on Learning Representations*. <https://openreview.net/forum?id=r1ecqn4YwB>.

Palmer, S. E. (1999). *Vision science: Photons to phenomenology*. MIT Press.

Petropoulos, F., Apiletti, D., Assimakopoulos, V., Babai, M. Z., Barrow, D. K., Ben Taieb, S., Bergmeir, C., Bessa, R. J., Bijak, J., Boylan, J. E., Browell, J., Carnevale, C., Castle, J. L., Cirillo, P., Clements, M. P., Cordeiro, C., Cyrino Oliveira, F. L., De Baets, S., Dokumentov, A., ... Ziel, F. (2022). Forecasting: Theory and practice. *International Journal of Forecasting*, 38(3), 845–1154.

Pincus, S. M. (1991). Approximate entropy as a measure of system complexity. *Proceedings of the National Academy of Sciences*, 88(6), 2297–2301.

Richman, J. S., & Moorman, J. R. (2000). Physiological time-series analysis using approximate entropy and sample entropy. *American Journal of Physiology-Heart and Circulatory Physiology*, 278(6), H2039–H2049.

Seabold, S., & Perktold, J. (2010). Statsmodels: Econometric and statistical modeling with Python. In *Proceedings of the 9th Python in Science Conference* (pp. 57–61). SciPy.

Shannon, C. E. (1948). A mathematical theory of communication. *Bell System Technical Journal*, 27(3), 379–423.

Stock, J. H., & Watson, M. W. (2003). Forecasting output and inflation: The role of asset prices. *Journal of Economic Literature*, 41(3), 788–829.

Tiao, G. C., & Tsay, R. S. (1994). Some advances in non-linear and adaptive modelling in time-series. *Journal of Forecasting*, 13(2), 109–131.

Wang, R., Klee, S., & Roos, A. (2025). Time series forecastability measures. In *Proceedings of the 1st Workshop on "AI for Supply Chain: Today and Future" @ 31st ACM SIGKDD Conference on Knowledge Discovery and Data Mining (KDD '25)*. ACM.